Biochemical and Biophysical Research Communications 427 (2012) 525–530

Contents lists available at SciVerse ScienceDirect

Biochemical and Biophysical Research Communications

journal homepage: www.elsevier.com/locate/ybbrc

Visualizing the mouse podocyte with multiphoton microscopy

Charbel C. Khoury [a,*,1], Mark F. Khayat [a,*,1], Tet-Kin Yeo [a], Petr E. Pyagay [a], Amy Wang [a], Allan M. Asuncion [b], Kumar Sharma [b], Weiming Yu [c], Sheldon Chen [a]

[a] Division of Nephrology/Hypertension, Northwestern University, Chicago, IL, USA
[b] Center for Renal Translational Medicine, University of California, San Diego, La Jolla, CA, USA
[c] Department of Physiology, Northwestern University, Chicago, IL, USA

ARTICLE INFO

Article history:
Received 27 August 2012
Available online 26 September 2012

Keywords:
Green fluorescent protein
2-Photon microscopy
Podocyte processes
Renal corpuscle

ABSTRACT

The podocyte is a highly specialized kidney glomerular epithelial cell that plays an essential role in glomerular filtration and is believed to be the target of numerous glomerular diseases leading to proteinuria. Despite the leaps in our understanding of podocyte biology, new methodologies are needed to facilitate research into the cell. Multiphoton microscopy (MPM) was used to image the nephrin knockout/green fluorescent protein (GFP) knock-in heterozygote (*Nphs1*^{tm1Rkl}/J) mouse. The nephrin promoter restricts GFP expression to the podocytes that fluoresce green under excitation. From the exterior of an intact kidney, MPM can peer into the renal parenchyma and visualize the podocytes that outline the globular shape of the glomeruli. Details as fine as the podocyte's secondary processes can be resolved. In contrast, podocytes exhibit no fluorescence in the wildtype mouse and are invisible to MPM. Phenotypically, there are no significant differences between wildtype and *Nphs1*^{tm1Rkl}/J mice in body weight, urinary albumin excretion, creatinine clearance, or glomerular depth. Interestingly, the glomeruli are closer to the kidney capsule in female mice, making the gender the preferred choice for MPM. For the first time, green fluorescent podocytes in a mouse model free of confounding phenotypes can be visualized unequivocally and in the "positive" by MPM, facilitating intravital studies of the podocyte.

1. Introduction

Proteinuria is a growing health concern. It reflects worsening kidney disease and is an independent risk factor for cardiovascular morbidity and mortality. Whether due to primary glomerular diseases or antibody-mediated insults or metabolic diseases, proteinuria has generally been ascribed to some form of podocyte dysfunction [1]. Justifiably, the podocyte has become a favored topic of researchers in the field. This highly specialized epithelial cell extends primary processes that cover the glomerular capillaries and branch into thinner secondary foot processes or pedicels. The pedicels anchor the podocyte to the glomerular basement membrane and interdigitate with neighboring foot processes to form the slit diaphragm. Despite major advances in our understanding of the cell's molecular mechanisms, the podocyte remains a relatively mysterious cell.

Multiphoton fluorescence excitation microscopy (MPM) has become an important tool in the study of renal physiology and has seen an exponential increase in its applications over the past decade [2–7]. By using near-infrared lasers, this "non-linear" imaging technique collects optical sections deep into tissues and allows the detection of fluorescent signals, with high resolution and down to the subcellular level [8]. Since it causes minimal phototoxicity, MPM is an ideal methodology to image cells, such as the podocyte, in their native tissue/organ environment. This would complement the current mainstays of podocyte research techniques, i.e., cell biology and pathology. Nonetheless, the main limitation of MPM in the kidney is the depth limit of imaging. The high refractive index heterogeneity of renal tissue results in substantial scattering of light and the generation of widespread out-of-focus fluorescence. That combined with the effect of spherical aberration, scattering, and the partial absorption of light by hemoglobin has limited the reach of MPM into the kidney to a maximum of 150–200 μm [9,10]. Since the majority of mouse glomeruli normally lie at or below this depth limit, MPM of the podocyte in the mouse has been difficult. We report the successful imaging of podocytes in nephrin knockout/green fluorescent protein (GFP) knock-in heterozygous female mice. These mice have normal glomerular structure and function but gain a podocyte-specific GFP expression under the nephrin promoter [11]. We believe that this model could potentially be used to follow the activities of the podocyte in health and disease.

* Corresponding authors.
E-mail addresses: khoury.charbel@gmail.com (C.C. Khoury), m-khayat@northwestern.edu (M.F. Khayat).
[1] These authors contributed equally to the work.

0006-291X/$ - see front matter © 2012 Elsevier Inc. All rights reserved.
http://dx.doi.org/10.1016/j.bbrc.2012.09.089

2. Materials and methods

2.1. Animals and reagents

Female nephrin knockout/GFP knock-in heterozygote *Nphs1*^{tm1Rkl}/J mice [11] and both genders of B6129SF2/J strain-matched control mice were acquired from Jackson Laboratory (stock number: 005692) at 6–8 weeks of age. Male *Nphs1*^{tm1Rkl}/J mice were created by breeding. Genetically-modified and control mice were imaged from 7 to 20 weeks of age. Animal protocols were approved by the Animal Care and Use Committee of Northwestern University and were in compliance with the National Institutes of Health Guide for the Care and Use of Laboratory Animals. Fluorescent reagents used for imaging were 500-kDa Texas Red-conjugated dextran (Sigma, St. Louis, MO, USA).

2.2. Urinary albumin excretion and creatinine clearance

Urinary albumin excretion and creatinine clearance were measured at 6, 8, 12, 16, and 20 weeks of age. From the retro-orbital sinus, blood was collected and processed into plasma that was stored at −80 °C until analysis. Plasma creatinine concentrations were then determined by high-performance liquid chromatography (HPLC) as previously described [12]. An 18-h urine collection was done for each mouse. Urinary creatinine concentrations were measured with the Creatinine Companion kit (Exocell, Philadelphia, PA, USA), and creatinine clearances were calculated by the standard clearance equation. Urinary albumin concentrations were measured by an enzyme-linked immunosorbent assay (ELISA) kit (AssayPro, St. Charles, MO, USA) specific for mouse albumin, and the urinary albumin excretion rate was extrapolated to 24 h.

2.3. Quantification of glomerular depth

Kidney samples for routine histological analysis and glomerular depth measurements were obtained from 12-week-old mice. Following deep anesthesia with isoflurane and euthanasia of the mice by cervical dislocation, the kidneys were excised and fixed in 4% paraformaldehyde, embedded in paraffin, and sectioned into 5-μm sections. Hematoxylin and eosin staining was performed with a standard protocol. To assess the proximity of the glomeruli to the renal capsule, stained paraffin sections were photographed under a light microscope and the shortest distance between the glomerular tuft border and the renal capsule was measured using the Image J measuring tool. Every glomerulus within 200 μm of the capsule was counted over the entire circumference of a mid-coronal kidney section. Glomeruli greater than 200 μm from the capsule were discarded from depth measurement analysis.

2.4. Imaging ex vivo kidney tissue

To image intact kidneys, mice were anesthetized with isoflurane initially, followed by an intraperitoneal injection of ketamine/xylazine (100 mg/kg: 10 mg/kg). The retroorbital sinus was injected with 500 μl of Texas Red-conjugated dextran (500,000 mol. wt., 3.25 mg/ml in PBS) and a few minutes were waited to allow the fluorescent dextran to circulate into the kidneys and throughout the body. While under deep anesthesia, the mouse was euthanized by cervical dislocation. The abdominal cavity was exposed, the kidneys were dissected free, and the renal pedicle was clamped with 1 mm wide microclips, exerting 70 g of pressure (Roboz, Gaithersburg, MD, USA), in order to trap the Texas Red dextran. The kidney was excised with its capsule intact and kept in phosphate-buffered saline (PBS) on ice. Imaging of the kidney was started within 30 min of extraction.

Kidneys were imaged using an FV1000MPE microscope system (Olympus, Center Valley, PA, USA) that was designed for multiphoton imaging. The system is equipped with the Titanium–Sapphire Mai Tai DeepSee HP laser with an integrated 14 W pump Millennia laser (Spectra-Physics, Santa Clara, CA, USA), an acousto-optic modulator (AOM) attenuator, and a Keplerian-style collimator/beam expander. The illumination path was aligned using a fluorescent slide to center the beam and the point-spread functions of 2.2 μm green beads (Olympus, Center Valley, PA, USA) and 6.2 μm multiple-labeled beads (Spherotech, Lake Forest, IL, USA) mounted on a cover slip. Images were collected using the XLPLN 25× W MP water dipping objective (Olympus) with Numerical Aperture of 1.05. Z-stack images were produced by taking 512 × 512-pixel images in 2.39 μm steps to a depth of around 220 μm from the renal capsule. The pixel dwell time was 8.0 μs, and lines were Kalman-averaged 2×. Excitation wavelengths used were 860 nm, 920 nm, or 940 nm for detecting different combinations of kidney autofluorescence, second harmonic generation, GFP, and Texas Red. Fluorescence saturation was avoided. Image processing was done with ImageJ and Volocity.

2.5. Statistical analyses

Quantitative data are presented as scatter plots with the line indicating the median value or as graphs depicting the arithmetic mean ± SEM. Statistical significance, defined at a P value < 0.05, was determined using one-way Analysis of Variance (ANOVA) with the Bonferroni correction.

3. Results

3.1. GFP-podocytes delineate glomeruli

To analyze the feasibility of the nephrin knockout/GFP knock-in heterozygote mouse as a model for podocyte imaging, we used freshly explanted kidneys, making sure to maintain the integrity of the renal capsule. With the excitation wavelength set at 860 nm, we collected serial z-stack images of the renal cortex reaching a maximum depth of around 220 μm from the kidney surface (Movie S1 in supporting information). Tubules are seen first; they are visible because of autofluorescence. As MPM looks deeper inside the kidney, glomeruli are detected in the green channel, appearing as round corpuscles that can be clearly distinguished from the surrounding tubules (Fig. 1). No bleed-through was detected in the red and blue channels, confirming the signal to be true GFP fluorescence (data not shown). Furthermore, the average diameter of the glomeruli is ~65 μm, consistent with previous observations and keeping in mind that the outer cortical glomeruli are typically smaller than juxtamedullary ones and that female glomeruli tend to have a smaller volume than their male counterparts [13].

By using second harmonic generation (SHG) to demarcate the renal capsule by its collagen fibers, we determined that glomeruli become visible at ~60 μm away from the *Nphs1*^{tm1Rkl}/J kidney surface in female mice. A montage of a z-series from superficial to deep is shown (Fig. 1). Collagen fibers are shown arbitrarily in blue, while the green channel detects the GFP signal from podocytes as well as autofluorescence from tubular cells. In contrast, we could not image any glomeruli from the surface of intact kidneys of B6129SF2/J control mice. The podocytes in wildtype mice display no fluorescence, unlike in the *Nphs1*^{tm1Rkl}/J mice.

3.2. Female mice have glomeruli closer to the kidney surface

Glomerular depth was investigated further to calibrate our expectations of the number of glomeruli that can be reached by

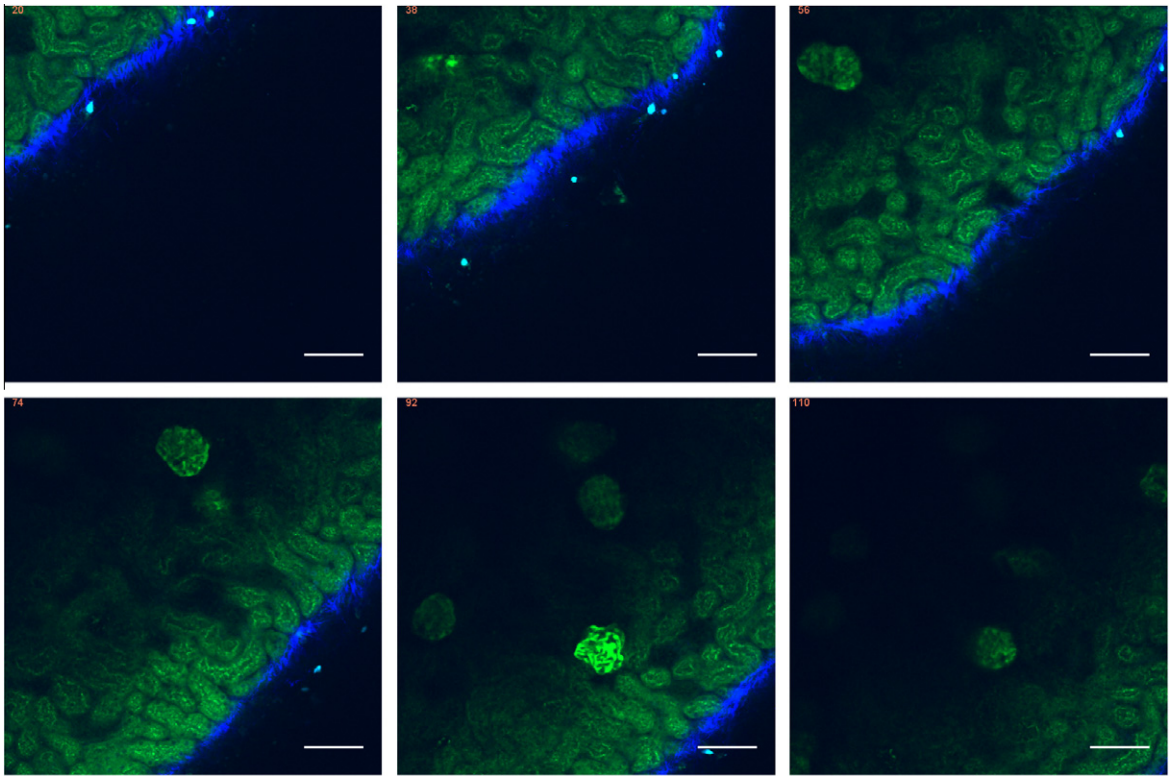

Fig. 1. MPM can directly image glomeruli with GFP signal emanating from the podocytes. Shown here is a montage of multiphoton microscopy z-series collected from the surface of an intact *Nphs1*^{tm1Rkl}/J mouse kidney. GFP and tubular autofluorescence appear in the green channel. Second harmonic generation delineates collagen fibers in the renal capsule, depicted in blue. As MPM penetrates deeper into the kidney, the corpuscular-shaped glomeruli come into view. *Nphs1*^{tm1Rkl}/J glomeruli are as close as 60 μm from the renal capsule. Stack number is noted in the left upper corner. Pixel dimensions are 0.497 × 0.497 μm. Scale bar is 50 μm. The full z-series is available in the supporting information (Movie S1).

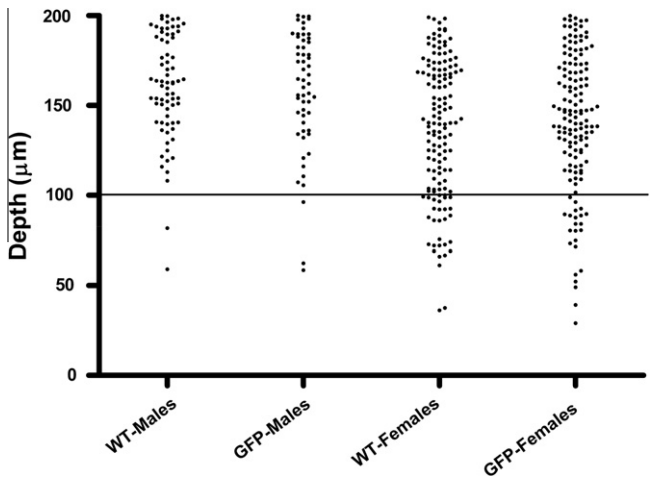

Fig. 2. Glomerular depth assessed by H&E on mid-coronal kidney sections. All glomeruli around the perimeter of the stained kidney sections that were less than 200 μm from the renal capsule were counted and are displayed in the scatter plot according to their depth. All four mouse groups at 12 weeks of age ($N = 3$ per group) were analyzed. A line is arbitrarily drawn at 100 μm, because up to that depth the glomeruli could be easily visualized by our MPM system. In comparing wildtype to *Nphs1*^{tm1Rkl}/J mice, there are no significant differences in the glomerular depths between the two male groups and two female groups. Comparing males to females, regardless of genotype, the females have a greater abundance of glomeruli that fall within the 100-μm distance. Thus, only females were used for MPM imaging.

MPM. A comprehensive surveillance of glomerular distance from the kidney capsule was undertaken by H&E staining of paraffin sections. The surveillance was capped at 200 μm, the depth that MPM can feasibly penetrate into the kidney. There are no differences in the distribution of glomeruli within 200 μm of the renal capsule between the wildtype and *Nphs1*^{tm1Rkl}/J mice (Fig. 2). The nephrin-GFP knock-in does not appear to cause a renal developmental defect or thinning of the cortex. However, the number of shallow glomeruli (<100 μm from the capsule) was higher in females vs. males, regardless of the genotype. We surmise that because the female kidney is globally smaller in size, it is statistically more likely to have glomeruli at the shallower depths. Biological factors related to gender may also play a role. At least in this mouse strain, females are easier to visualize by MPM for the podocytes.

3.3. MPM brings out podocyte detail in an intact kidney

The GFP signal imbues much of the podocyte expanse, allowing the primary processes to be easily seen as they extend from the cell body. In some cases, secondary processes can be visualized (Fig. 3A). The glomeruli perfused with 500-kDa Texas Red-conjugated dextran show the relationship of the podocytes to the capillaries (Fig. 3D). At no time does the green fluorescence of the podocyte overlap with the red fluorescence of the capillary, consistent with the fact of their spatial discreteness.

3.4. Characterization of the *Nphs1*^{tm1Rkl}/J mouse

The *Nphs1*^{tm1Rkl}/J mice, both male and female, were characterized from 6 to 20 weeks of age. The body weights all increased with age, and males were significantly heavier than females. Comparing wildtype to *Nphs1*^{tm1Rkl}/J mice, the body weight is not significantly different (Fig. S1 in supporting information), demonstrating that the knock-in of GFP into one nephrin allele does not cause a gross bodily phenotype.

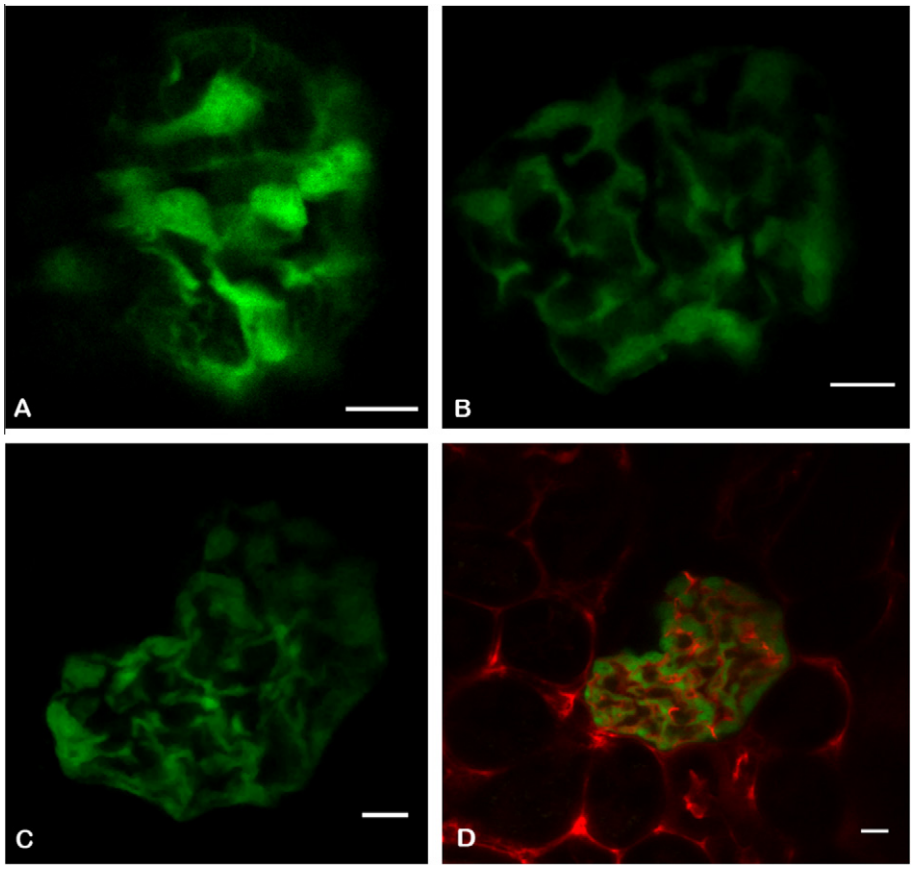

Fig. 3. MPM brings out podocyte details in the *Nphs1*^{tm1Rkl}/J mouse. Panels A–C show the green fluorescent podocytes alone. Details of the podocyte primary processes and hints of the secondary processes can be discerned. Panel D shows the podocytes plus the perfused 500-kDa Texas Red dextran that outlines the capillaries, highlighting the podocytes' spatial relationship to the glomerular capillaries. Scale bar is 10 μm.

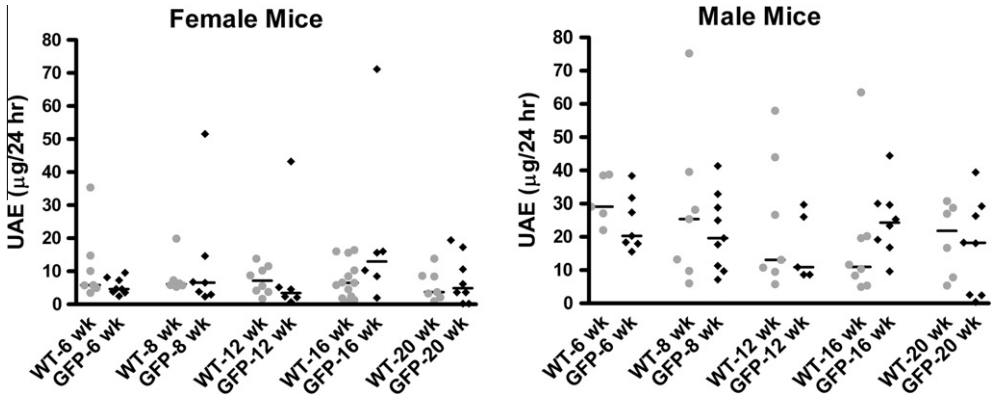

Fig. 4. 24-h Urinary albumin excretion (UAE) in the mouse groups. Scatter plots depict individual-level data on UAE for each of the mice according to the genotype (WT vs. GFP) and age (6, 8, 12, 16, and 20 weeks of age). The bar represents the median value of the 24-h UAE within each group. No difference was detected between wildtype and *Nphs1*^{tm1Rkl}/J mice. Within each gender, the genotype did not influence the degree of albuminuria. P = NS for WT vs. GFP. However, within the wildtype group, females had less albuminuria than males. $P < 0.001$ for males vs. females.

To examine whether the GFP knock-in/nephrin knockout in *Nphs1*^{tm1Rkl}/J mice manifests a renal phenotype, we measured 24-h urine albumin excretion (UAE) and creatinine clearance at 6, 8, 12, 16, and 20 weeks of age. Albuminuria did not increase as the animals aged (Fig. 4). Females, both wildtype and *Nphs1*^{tm1Rkl}/J, had less albuminuria than the male wildtypes, though no difference in albuminuria was seen between the two female genotypes or between female and male *Nphs1*^{tm1Rkl}/J mice. Most importantly, albuminuria within each age and gender combination did not differ between wildtype and *Nphs1*^{tm1Rkl}/J mice (Fig. 4). Kidney function, assessed by the creatinine clearance, also was unchanged at each age group and by gender when comparing wildtype and *Nphs1*^{tm1Rkl}/J mice (Fig. S2 in supporting information). Males tended toward a higher creatinine clearance than the females, but the difference was not significant. Thus, the genetic modification that specifically endows podocytes with GFP fluorescence does not introduce a confounding phenotype or an overt glomerular impairment.

4. Discussion

Until now, MPM imaging of the podocyte has been mostly limited to the Munich-Wistar rat because of its superficial glomeruli. In mice with deeper glomeruli, the work-around has been to surgically expose the kidney cortex. The use of the female *Nphs1*^{tm1Rkl}/J mouse solves this problem by having glomeruli that are superficially located. The other distinct advantage of the *Nphs1*^{tm1Rkl}/J mouse, one that is particularly suited for multiphoton microscopy, is that the podocytes possess an endogenous fluorescence, allowing their direct imaging "in the positive." This contrasts with techniques applied in the Munich-Wistar rat in which the podocyte has been visualized "in the negative." Briefly, all glomerular structures and fluid spaces except for the podocyte [and glomerular basement membrane (GBM)] were fluorescently labeled [14]. In this way, the dark unlabeled podocyte stood out between the rhodamine fluorescence in the capillary and the Lucifer yellow fluorescence in the urinary space. In comparison, the *Nphs1*^{tm1Rkl}/J mouse obviates most of the indirectness by specifically labeling only the podocyte with GFP, according to the genetic program of the nephrin promoter. Accordingly, the podocyte is imaged "positively," and none of the endothelial, mesangial, or parietal epithelial cells display a significant signal in the green channel (Fig. 3).

Intravital multiphoton microscopy can be used to study various aspects of podocyte physiology and pathophysiology. Once our mouse model is adapted to intravital MPM, the live imaging in real time will enrich the analysis of podocyte behavior. If podocyte phenomena occur slowly, serial investigations can be performed in a single mouse. Recent intravital experiments in the rat by Peti-Peterdi brought forth live evidence of podocytes detaching from the GBM and subsequently being replaced by parietal epithelial cells [14,15]. It would be interesting to test those findings in this mouse model. Since the parietal epithelial cells do not express GFP in the *Nphs1*^{tm1Rkl}/J mouse, their transformation into podocytes could be more clearly perceived. However, it is possible that the parietal cell, in becoming a podocyte, will eventually activate the nephrin promoter and start to express GFP.

While it is generally accepted that the podocyte regulates the permselectivity of the glomerulus, whether it does so by maintaining a rigid cytoarchitecture or fluidly adjusting to the demands of filtration has not been fully examined. The podocytes may yet comprise a more responsive and fluctuating landscape than previously believed, and the ramifications of podocyte motion can be further analyzed with respect to proteinuria in kidney diseases. Evidence of podocyte dynamism was demonstrated in podocytes that could migrate along the capillary loop, a property that had only been suspected based on cell culture motility findings [16–18]. Though controversial still, the putative podocyte movement can be confirmed and characterized in the *Nphs1*^{tm1Rkl}/J imaging model where the identity of the podocyte is unambiguous.

Other potential podocyte roles could be further explored and would benefit from MPM imaging of the *Nphs1*^{tm1Rkl}/J mouse. How do podocytes evolve in appearance when they detach and/or apoptose? The events leading up to a dearth of podocyte density, which is characteristic of several proteinuric renal diseases, might be trackable over time [19,20]. The cell's function in the maintenance of the subpodocyte space and the cleaning of the glomerular filter are receiving increased attention [21,22]. Post-renal transplant podocyte and glomerular changes, previously eluding visualization by MPM due to a scarcity of glomeruli near the renal capsule, can now be recorded [23]. Perhaps these phenomena can be clarified by pairing the ability to track fluorescent podocytes with existent techniques to measure GFR via fluorescent markers [24,25]. We may one day be able to evaluate the effect of a podocyte morphology change upon single nephron GFR and macromolecular permeability.

In conclusion, this is the first time, to our knowledge, that innately fluorescent podocytes have been imaged by multiphoton microscopy in an intact mouse kidney, made all the more feasible by the fortuitous proximity of the glomeruli to the kidney capsule in the female mouse. Together with intravital multiphoton microscopy, the opportunity to visualize and quantify podocyte structure and function using the *Nphs1*^{tm1Rkl}/J mouse, both in real time and in the native glomerular environment, will augment the study of the podocytopathies. The fluorescent podocyte mouse model is also amenable to the induction of glomerular diseases by exogenous agents, manipulations, or endogenous processes. Adding a visual facet to these established disease models would yield a fresh perspective, open up further lines of investigation, and reveal more about the nature of the enigmatic podocyte.

Acknowledgments

The authors wish to thank the following people for their contributions: Teng-Leong Chew of the Northwestern University Cell Imaging Facility negotiated the Olympus multiphoton microscope for public use and gave expert advice on image analysis. Satya Khuon and Constadina Arvanitis of the Chew lab also aided us greatly. James Lopez of Olympus provided expert guidance in acquiring the kidney images with the Olympus multiphoton microscope. Satish Ramachandra Rao of UCSD assisted in the HPLC creatinine assay development. Finally, Janos Peti-Peterdi of the University of Southern California has given generously of his feedback and collaborative time. The authors have no financial conflicts of interests.

Appendix A. Supplementary data

Supplementary data associated with this article can be found, in the online version, at http://dx.doi.org/10.1016/j.bbrc.2012.09.089.

References

[1] F.N. Ziyadeh, G. Wolf, Pathogenesis of the podocytopathy and proteinuria in diabetic glomerulopathy, Curr. Diabetes Rev. 4 (2008) 39–45.
[2] K.W. Dunn, R.M. Sandoval, B.A. Molitoris, Intravital imaging of the kidney using multiparameter multiphoton microscopy, Nephron Exp. Nephrol. 94 (2003) e7–e11.
[3] J. Peti-Peterdi, J.L. Burford, M.J. Hackl, The first decade of using multiphoton microscopy for high-power kidney imaging, Am. J. Physiol. Renal Physiol. 302 (2012) F227–F233.
[4] X. Li, W. Yu, Deep tissue microscopic imaging of the kidney with a gradient-index lens system, Opt. Commun. 281 (2008) 1833–1840.
[5] J. Peti-Peterdi, I. Toma, A. Sipos, S.L. Vargas, Multiphoton imaging of renal regulatory mechanisms, Physiology (Bethesda) 24 (2009) 88–96.
[6] S.L. Ashworth, R.M. Sandoval, G.A. Tanner, B.A. Molitoris, Two-photon microscopy: visualization of kidney dynamics, Kidney Int. 72 (2007) 416–421.
[7] B.A. Molitoris, R.M. Sandoval, Intravital multiphoton microscopy of dynamic renal processes, Am. J. Physiol. Renal Physiol. 288 (2005) F1084–F1089.
[8] W.R. Zipfel, R.M. Williams, W.W. Webb, Nonlinear magic: multiphoton microscopy in the biosciences, Nat. Biotechnol. 21 (2003) 1369–1377.
[9] P.A. Young, S.G. Clendenon, J.M. Byars, R.S. Decca, K.W. Dunn, The effects of spherical aberration on multiphoton fluorescence excitation microscopy, J. Microsc. 242 (2011) 157–165.
[10] P.A. Young, S.G. Clendenon, J.M. Byars, K.W. Dunn, The effects of refractive index heterogeneity within kidney tissue on multiphoton fluorescence excitation microscopy, J. Microsc. 242 (2011) 148–156.
[11] Y. Hamano, J.A. Grunkemeyer, A. Sudhakar, M. Zeisberg, D. Cosgrove, R. Morello, B. Lee, H. Sugimoto, R. Kalluri, Determinants of vascular permeability in the kidney glomerulus, J. Biol. Chem. 277 (2002) 31154–31162.
[12] S.R. Dunn, Z. Qi, E.P. Bottinger, M.D. Breyer, K. Sharma, Utility of endogenous creatinine clearance as a measure of renal function in mice, Kidney Int. 65 (2004) 1959–1967.
[13] I.J. Murawski, R.W. Maina, I.R. Gupta, The relationship between nephron number, kidney size and body weight in two inbred mouse strains, Organogenesis 6 (2010) 189–194.
[14] J. Peti-Peterdi, A. Sipos, A high-powered view of the filtration barrier, J. Am. Soc. Nephrol. 21 (2010) 1835–1841.

[15] D. Appel, D.B. Kershaw, B. Smeets, G. Yuan, A. Fuss, B. Frye, M. Elger, W. Kriz, J. Floege, M.J. Moeller, Recruitment of podocytes from glomerular parietal epithelial cells, J. Am. Soc. Nephrol. 20 (2009) 333–343.
[16] E.Y. Lee, C.H. Chung, C.C. Khoury, T.K. Yeo, P.E. Pyagay, A. Wang, S. Chen, The monocyte chemoattractant protein-1/CCR2 loop, inducible by TGF-beta, increases podocyte motility and albumin permeability, Am. J. Physiol. Renal Physiol. 297 (2009) F85–F94.
[17] B. George, B. Vollenbroker, M.A. Saleem, T.B. Huber, H. Pavenstadt, T. Weide, GSK3{beta} inactivation in podocytes results in decreased phosphorylation of p70S6K accompanied by cytoskeletal rearrangements and inhibited motility, Am. J. Physiol. Renal Physiol. 300 (2011) F1152–F1162.
[18] S. Babayeva, Y. Zilber, E. Torban, Planar cell polarity pathway regulates actin rearrangement, cell shape, motility, and nephrin distribution in podocytes, Am. J. Physiol. Renal Physiol. 300 (2011) F549–F560.
[19] B.L. Wharram, M. Goyal, J.E. Wiggins, S.K. Sanden, S. Hussain, W.E. Filipiak, T.L. Saunders, R.C. Dysko, K. Kohno, L.B. Holzman, R.C. Wiggins, Podocyte depletion causes glomerulosclerosis: diphtheria toxin-induced podocyte depletion in rats expressing human diphtheria toxin receptor transgene, J. Am. Soc. Nephrol. 16 (2005) 2941–2952.
[20] M.W. Steffes, D. Schmidt, R. McCrery, J.M. Basgen, Glomerular cell number in normal subjects and in type 1 diabetic patients, Kidney Int. 59 (2001) 2104–2113.
[21] A.H. Salmon, I. Toma, A. Sipos, P.R. Muston, S.J. Harper, D.O. Bates, C.R. Neal, J. Peti-Peterdi, Evidence for restriction of fluid and solute movement across the glomerular capillary wall by the subpodocyte space, Am. J. Physiol. Renal Physiol. 293 (2007) F1777–F1786.
[22] C.R. Neal, P.R. Muston, D. Njegovan, R. Verrill, S.J. Harper, W.M. Deen, D.O. Bates, Glomerular filtration into the subpodocyte space is highly restricted under physiological perfusion conditions, Am. J. Physiol. Renal Physiol. 293 (2007) F1787–F1798.
[23] G. Camirand, Q. Li, A.J. Demetris, S.C. Watkins, W.D. Shlomchik, D.M. Rothstein, F.G. Lakkis, Multiphoton intravital microscopy of the transplanted mouse kidney, Am. J. Transplant. 11 (2011) 2067–2074.
[24] W. Yu, R.M. Sandoval, B.A. Molitoris, Rapid determination of renal filtration function using an optical ratiometric imaging approach, Am. J. Physiol. Renal Physiol. 292 (2007) F1873–F1880.
[25] W. Yu, Quantitative microscopic approaches for studying kidney functions, Nephron Physiol. 103 (2006) 63–p70.